Deep-seated gravitational slope deformation at Handcar Peak in the southern Coast Mountains of British Columbia

Gabe Hensold[1], Doug Stead[1] & John Clague[1]
[1]*Department of Earth Sciences, Simon Fraser University, Burnaby, British Columbia*
Danilo Moretti[2] & Matthieu Sturzenegger[1]
[2]*Dipartimento di Scienze della Terra e Geologico-Ambientali, Università di Bologna, Italy*

ABSTRACT
Deep-seated gravitational deformation of rock slopes is a common form of mass movement in the mountains of western Canada. This phenomenon is well displayed on the southwest face of Handcar Peak, in the southern Coast Mountains 38 km northwest of Pemberton, British Columbia. Taken together, data from geomorphological field mapping, a study of trench sediments, and numerical modeling indicate a complex failure mechanism triggered by debuttressing of the oversteepened valley side during deglaciation. Linear features such as antislope and normal scarps are the surface expression of movement on pre-existing weak fault planes.

RÉSUMÉ
Le sackung est une forme fréquente de mouvement de masse rocheuse dans les montagnes du Canada occidental. Ce phénomène est visible sur la face sud-ouest de Handcar Peak, dans le sud de la Chaîne Côtière, 38 km au nord-ouest de Pemberton, Colombie-Britannique. Des données obtenues lors d'une étude géomorphologique et la description de sediments le long d'une tranchée, ainsi que des résultats de modélisation numérique suggèrent un mécanisme de glissement complexe, déclenché par décompression post-glaciaire le long du versant escarpé de la vallée. En surface, des linéaments de type escarpements normaux à contre-pente, témoignent du mouvement en profondeur le long de failles préexistantes.

1 INTRODUCTION

Deep-seated gravitational slope deformation (DSGSD) is a well-documented type of rock slope failure characterized by (1) extremely to very slow movement (0.5-80 mm/yr), (2) total displacements that are much smaller than the size of the deforming rock mass, (3) common absence of a discrete, through-going basal shear plane, (4) large size (> 1 million m^3), and (5) surface linear features such as trenches, closed depressions, and uphill-facing scarps. This type of deformation is known in the literature by several other names, notably deep creep, gravitational spreading, and sackungen (Soldati 2004). It has been identified in many alpine areas of the world (Bovis and Evans 1996, Ambrosi and Crosta 2006), and commonly is interpreted as a paraglacial phenomenon caused by oversteepening and subsequent debuttressing of glaciated valley slopes (Ballantyne 2002).

Extensive deep-seated gravitational slope deformation is occurring at Handcar Peak in the Coast Mountains of southwestern British Columbia (Fig. 1). Researchers have previously made a kinematic interpretation of the failure (Bovis and Evans 1996) and analyzed the sedimentary fill in a trench behind one of its antislope scarps (Lund 2002). However, the geomorphological features at Handcar Peak have not been described in detail and no geotechnical analysis of the deformation has been completed. The objective of our study was to obtain a more complete understanding of the timing and cause of deformation at Handcar Peak by integrating information gained from geomorphological field mapping and trench sediment analysis with engineering geological mapping and numerical modeling.

2 SITE DESCRIPTION

2.1 Location and Topography

The Handcar Peak DSGSD is located on the northeast side of the Lillooet River valley, 38 km northwest of the town of Pemberton, BC (Fig. 1). It spans a 7 km-wide section of slope, comprising the southwest flanks of a series of peaks between Railroad Creek and North Creek. The smaller tributary valleys of Sampson Creek and Buck Creek cut through the deforming rock mass, dividing it into three main sections, here termed the western, central, and eastern areas (Fig. 2). The deforming slope rises 1850-2080 m over a horizontal distance of 5-6 km from the floor of Lillooet valley to a maximum elevation of 2340 m asl at Handcar Peak and Locomotive Mountain. The average angle of the deforming slope is 22 degrees; the steepest portions, such as the southeast face of Handcar Peak, slope 30-35 degrees. The upper part of the deforming slope is relatively planar, but irregular undulating benches lie at its base. Sampson Creek is deflected 90 degrees where it meets these benches and flows 2 km laterally along the slope. There is also an 800 m-wide bench at about 1900 m asl on the easternmost section of the DSGSD, east of Buck Creek. There, the surface deformational features extend to the upper end of the bench, but the slope above it to Caboose Mountain, Locomotive Mountain, and Tender Mountain is apparently stable.

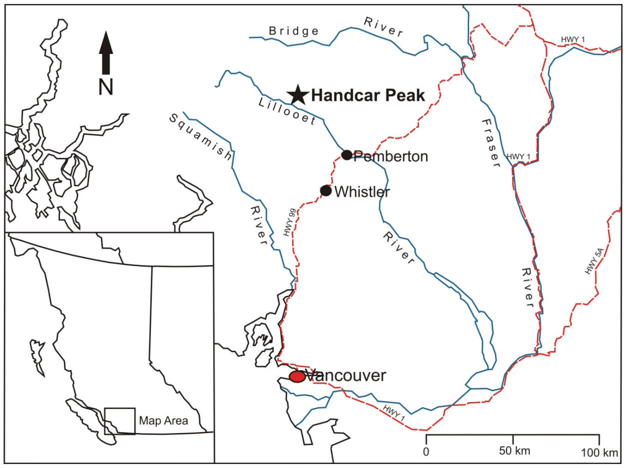

Figure 1. Location of Handcar Peak, southwestern British Columbia.

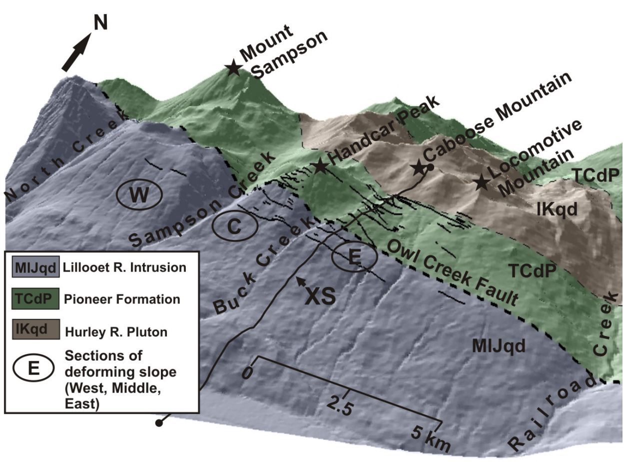

Figure 2. Topography and lithology of the Handcar Peak area. XS = line of cross-section shown in Fig. 5.

2.2 Lithology and Structure

The middle section of the deforming slope, where the linear surface features are most abundant, consists of metavolcanic rocks of the Pioneer Formation of the Cadwallader Group, an allocthonous island arc-related terrane (Monger and Journeay 1994). Near Handcar Peak, the Pioneer Formation comprises basaltic to rhyolitic porphyritic flows and tuffs metamorphosed to greenschist facies. To the northeast, the metavolcanic rocks have been intruded by late Cretaceous quartz diorite of the Hurley River Pluton, which forms the apparently stable upper part of the slope (Fig. 2).

The lower part of the deforming slope is late Jurassic quartz diorite of the Lillooet River Intrusion. The contact between this pluton and the Pioneer Group is the Owl Creek Fault, a northeast-dipping thrust created during a period of intense west-vergent contraction in the late Cretaceous (Monger and Journeay 1994). Narrow (1-3 m), southeast-striking, ductile shear zones that are possibly related to the Owl Creek Fault occur within the Pioneer Formation and are most common near the intrusive contact with the Hurley River Pluton. Small outcrops of altered quartz diorite are also found throughout the mapped area of the Pioneer Formation.

3 GEOMORPHOLOGY

The Handcar Peak slope displays classic morphological features of deep-seated gravitational movement, including lineaments, here termed ‘linears’ (antislope scarps, tension cracks, grabens, and double ridges), closed depressions and ponds, toe bulging, rockfall, and surficial instabilities contained within the larger deforming mass (Figure 3). Linears and related features were mapped using vertical aerial photographs. Mapping of the central and eastern parts of the DSGSD was checked in the field in the summer of 2009. The section west of Sampson Creek was not visited in the field due to difficult access and sparse deformation features.

3.1 Surface Features

Of the 77 linears mapped, 54 are antislope scarps, 16 are trenches or tension cracks, two are normal scarps, and five are composite forms (i.e. a combination of the other three features). Heights of antislope scarps range from approximately 0.3 to 15 m. Antislope scarps are most common on the steeper parts of the slope face, and trenches and tension cracks occur near the top of Handcar Peak and on the wide bench east of Buck Creek (Figure 4). The longest and straightest linears are oriented northwest-southeast, slightly oblique to the strike of the slope, and dip to the southeast. Some of the shorter linears, especially the trenches and tension cracks on the bench east of Buck Creek, intersect with each other, forming a laced pattern.

Linears displace hummocky late-Pleistocene deposits in the valley of Buck Creek, just east of Handcar Peak, and extend to the top of the 100-200-m-high scarp that forms the east margin of the valley (“Buck Creek Scarp” in Fig. 3). This relationship indicates that movement has occurred to at least a depth of 200 m in the rock mass, and probably deeper. The downhill extent of the deformation is less clearly defined. Typical DSGSD morphology involves linears in the upper part of the affected slope and a bulging area at the toe (Savage 1987, McCalpin 1999). Bovis and Evans (1996, p. 6) comment “Below scarp 1 [the lowest antislope scarp] are two prominent taluses associated with steep, downslope-bulging masses of what appear to be dilated, disintegrating rock…" No linears were identified in the field or on aerial photographs below this area, thus it may represent the lower limit of the deformation. However, the large irregular bench at the base of the mountainside, which displaces Sampson Creek, also appears to be bulged outwards, and its location corresponds with the section of the valley side that has linear surface features near the ridge top. These observations indicate that the deforming area may extend to the valley floor, which has been documented in some previous studies of DSGSD (Stewart 1997, Ambrosi and Crosta 2006). Figure 5 depicts both possibilities. Rockfall and small rockslides, some of which are fresh, are common around Handcar Peak (Fig. 3). Rockfall is concentrated below the steepened upper sides of linears on the southeast face of Handcar Peak, beneath a steep bulging zone below the lowermost major antislope scarp, and at the foot of Buck Creek Scarp. Six small rockslides were identified, all in areas of locally steep topography near antislope scarps or trenches. Two slides originated in the steep uphill walls of major trenches, and four occurred below antislope scarps.

3.2 Age of Activity

There are several signs of recent, and possibly continuing, movement at Handcar Peak, mainly in the upper part of the DSGSD. Linears on the main southeast face of Handcar Peak are intermittently buried by rockfall debris, and the steepest part of the rock mass above these features is fractured and dilated. The most recent rockslide ("fresh rockslide" on Fig. 3) also occurs in this area; a 50 m section of antislope scarp slid out on discontinuities that daylight on the downhill side of the scarp.

Evidence of recent activity east of Buck Creek is less obvious, but more directly indicative of deep-seated movement. Some of the trenches steepen at their base in the zone of laced intersecting linears (Fig. 4). Their convex profiles suggest recent, and probably continuing, spreading. Other clues that this area is actively extending include a 1-m-deep collapse pit at the base of one of the linears and an open tension crack approximately 2 m deep at the base of another.

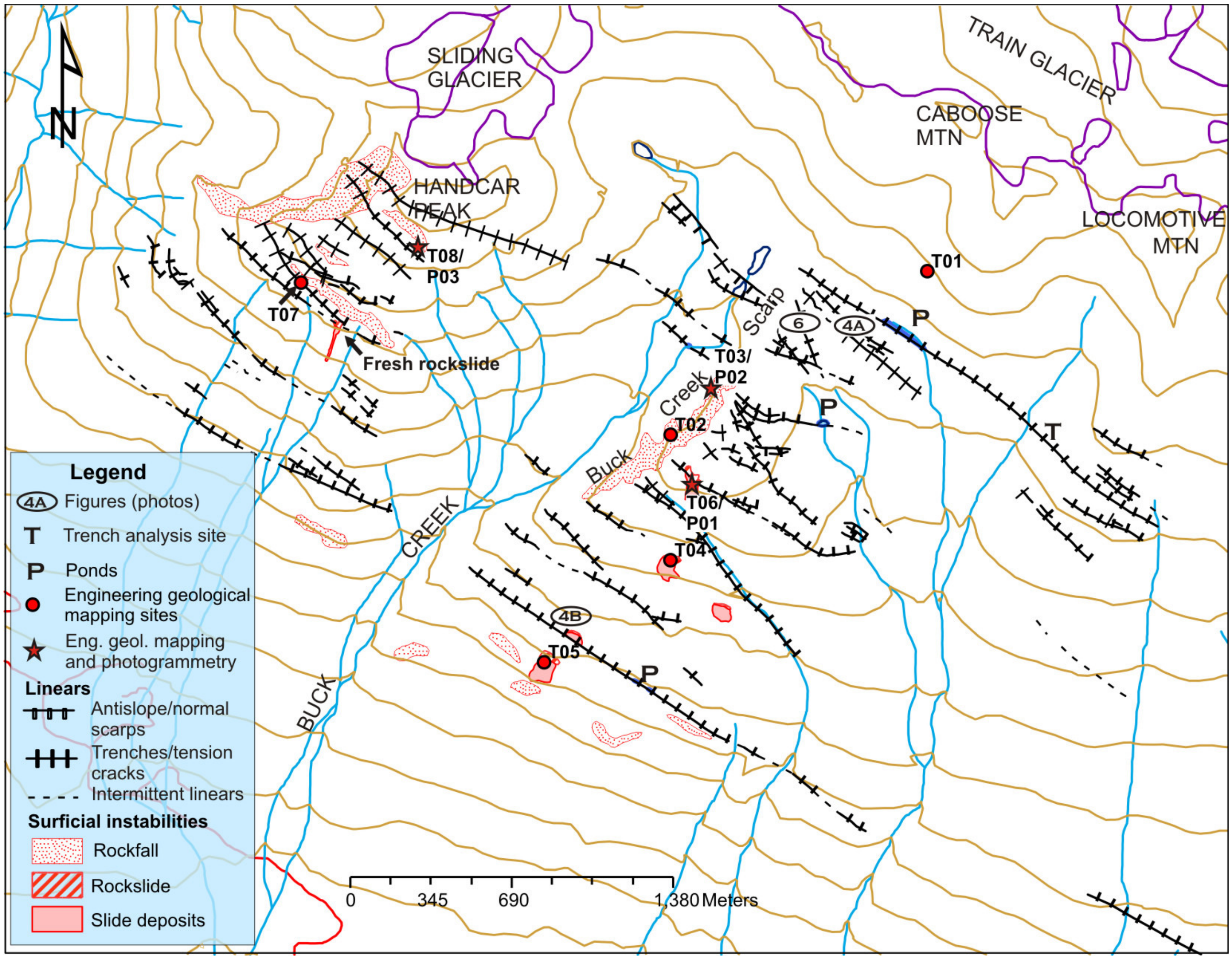

Figure 3. Surficial features, engineering geological mapping sites, and photo locations on the middle and eastern sections of the Handcar Peak DSGSD.

Figure 4. Linears. A: Trench with actively spreading tension crack at its base, looking northwest. B: Major antislope scarp in the eastern section of the deforming area, looking southeast.

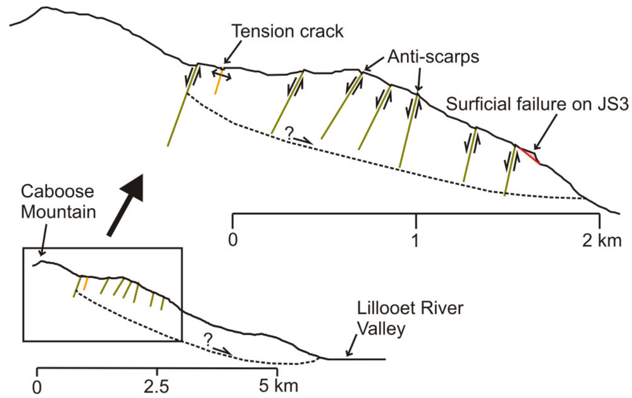

Figure 5. Schematic cross section of the slope east of Buck Creek (see Fig. 2 for location). Dashed lines are hypothesized lower limits of the deforming rock mass.

Figure 6. Traces of an anti-slope scarp (left) and normal scarp (right) displacing glacial drift in the valley of Buck Creek, looking NW. The normal scarp runs under a Little Ice Age moraine (red).

In contrast, there are few signs of recent movement along the lower antislope scarps. The depressions upslope of these scarps are filled with weathered colluvium and soil; they appear to have been stable for some time. The scarps of the four lower rockslides east of Buck Creek are covered with lichens and other plants, and appear to have occurred hundreds of years ago or more. The uppermost slide in this area is fresher than the others, but not as fresh as the slide on the southeast face of Handcar Peak. A conspicuous linear crosses Buck Creek valley but is covered by a Little Ice Age moraine on the west side of the valley; the moraine does not seem to have been displaced (Fig. 6).

4 TRENCH INVESTIGATION

A 6-m-long, 2-m-deep trench was dug through the sediment fill behind one of the major antislope scarps near the east end of the deforming area (see Fig. 3 for location). The site was chosen based on its morphological prominence and its relatively fine-grained, near-surface fill.

Four sediment units and three bedrock units were identified in the walls of the trench (Fig. 7). An inclined surface of highly fractured and weathered bedrock underlies the antislope scarp from the southwest end to the middle of the trench (Fig. 6 – Units A/B). In places, the rock is completely disaggregated into a loose regolith of angular sand-sized particles and larger clasts; the disaggregation is the result of recent movement on the scarp. The weathered bedrock surface is capped by a layer of massive red clay gouge approximately 10-15 cm thick (Unit C). The clay gouge delineates a fault with up to 2 m of dip-slip displacement; i.e. the amount of vertical relief on the antislope scarp.

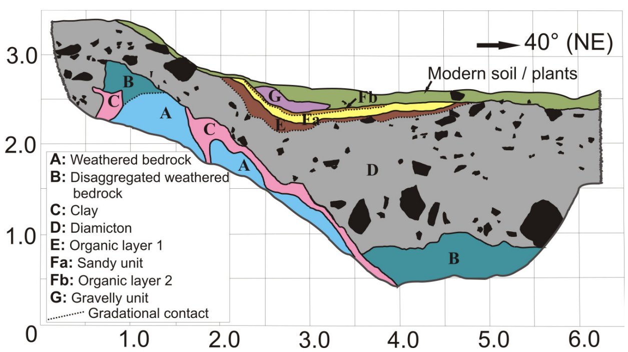

Figure 7. Sketch of northwest wall of trench, with interpreted lithologic units. The units on the vertical and horizontal axes are meters.

The fault scarp and bedrock at the base of the trench are overlain by a light brownish-grey, massive, matrix-supported diamicton (Unit D). The diamicton grades upward into a dark brown, fine to medium sand with minor subrounded gravel (Unit E), which we interpret to be a paleosol developed in the top of Unit D. Unit F sharply overlies unit E and comprises approximately 10 cm of loose, fine to medium sand. The uppermost 2-4 cm of the unit is dark yellowish-brown, a consequence of minor oxidation. The unit also contains abundant grains of volcanic glass derived from the eruption of Mount Meager ca. 2400 yrs ago (Clague et al. 1995). Unit F records inwash of sand into the trench shortly after the eruption. It is overlain by a lens, 75-cm wide, of subrounded to subangular gravel (Unit G).

Units F and G extend up onto the antislope scarp; they have been dropped downward and deformed by movement along the fault that coincides with the scarp. Assuming the two units were originally horizontal, approximately 0.5 m of vertical movement has occurred since 2400 yrs ago. The other 1.5 m of vertical displacement on the fault must have occurred between deglaciation and 2400 yrs ago.

We infer that movements on the fault delineating the antislope scarp are gravitational in origin. We also considered the possibility that the movements could be the result of episodic large earthquakes. The fault that created the antislope scarp was a tectonic fault some time in the past, because the clay gouge could not have been produced by gravitational displacements near the surface. However, several lines of evidence support a gravitational origin for this antislope scarp and other linears at Handcar Peak. First, the linears occur in more-or-less parallel sets, whereas earthquake-generated scarps are commonly individual features (McCalpin 1999). Second, most gravitational linears, like those at Handcar Peak, occur on the upper parts of high ridges and trend approximately parallel to the slope (McCalpin 1999). Third, displacements on the trenched antislope scarp occurred over the entire Holocene, and about 0.5 m of displacement has happened since 2400 years ago. Some of the nearby linears have fresh cracks indicative of continuing movement. Such lengthy and continuing movement is inconsistent with a seismic origin for the scarps.

5 GEOTECHNICAL STUDY

5.1 Data Collection

Rock mass data were collected at eight sites on the deforming slope (see Fig. 3 for locations). Rock mass quality was estimated using the Geological Strength Index (GSI) method (Hoek et al. 2002). Lithology, block size and shape, weathering grade, and relevant geologic structures were noted. Samples were collected for point load testing to determine the unconfined compressive strength (UCS) of the intact rock. Discontinuity surveys were conducted by spot mapping of joint sets, supplemented with photogrammetry-based mapping at three sites (Fig. 3). Photographs for photogrammetric analysis were taken with a Canon Rebel XTi digital SLR camera with an 18-55 mm zoom lens. Relative positions and orientations of the camera stations were measured in the field with a metric tape and a geologic compass. These measurements were later used to register the photogrammetry models (Sturzenegger and Stead 2009). Models were created and registered with the program 3DM CalibCam, and discontinuity mapping was done with 3DM Analyst (ADAM Technology 2007).

5.2 Rock Mass Characterization

GSI values of the rock mass at Handcar Peak, based on visual estimates of the rock mass blockiness (average block volume in cm^3) and joint surface quality, range from 50 to 70 and average 60. The blockiness index ranges from blocky to very blocky, and joint surface conditions are generally good to fair. Joint spacing differs from outcrop to outcrop, with block sizes in the range of 10^3 to 10^5 cm^3.

5.3 Discontinuity Characterization

Joint sets identified from spot mapping are shown in Figures 8A and 9. Set 1 (JS1), which is the most dominant, strikes northwest approximately parallel to the Owl Creek Fault and dips steeply into the slope. Its pole distribution is slightly bimodal, because it is steeper and more northerly striking in rocks on the west side of the Owl Creek Fault than on the east side. Some of the joints in JS1 have very high persistence, >20 m (International Society of Rock Mechanics 1978). Set 2 (JS2) is a sub-vertical set with persistence similar to JS1; it strikes from south to southwest, providing lateral release for downhill-directed movement. Set 3 (JS3) is a conjugate set to JS1, but appears as two separate clusters of poles on the stereonet. In metavolcanic rocks east of Buck Creek, the set dips 60 degrees on average (JS3' in Fig. 8A); in other areas, the dip is 30-45 degrees. In the vicinity of the lowest antislope scarps, JS3 daylights in locally steep outcrops as smooth and polished sliding planes. Set 4 (JS4) dips 20-40° towards the south to south-southeast. Its low persistence of 1-5 m and rough, undulating joint surfaces make it less liable to slide than JS3. Joint surfaces in all sets are slightly weathered (class II according to ISRM 1978).

The data obtained using photogrammetry-based mapping (Fig. 8B, 8C) do not correlate exactly with spot mapping data from the same sites, which highlights the fact that both methods contain some bias. Discontinuities in joint set 4 were less frequently identified in photogrammetric mapping, probably because their typically low persistence made them difficult to identify on photographs taken from a distance. Some anomalous joint set orientations are also emphasized in the photogrammetry data, because they happened to be particularly visible in some part of the mapped outcrop. This phenomenon probably accounts for the outlier set JS4' in Figure 8C. On the other hand, the wide natural range of joint set orientations within individual outcrops is not as well represented in the spot mapping data.

5.4 Kinematic Analysis

Toppling on a large scale is not kinematically possible at Handcar Peak (Fig. 8a), even assuming low discontinuity shear strength due to pore-water pressures. Sliding is possible under these conditions, although only on the shallowest discontinuities of joint sets 3 and 4 that daylight on the slope. In small cliff outcrops where the local slope can be as steep as 60 degrees, toppling on JS1 and sliding on JS3 and JS4 are possible. Wedge failure (not shown in Fig. 8) involving JS3 and JS4 can also occur locally in steep outcrops. Field observations indicate that planar sliding on JS3 is likely the cause of most of the surficial rockslide events described above. Figure 8c shows that the Buck Creek Scarp, which is perpendicular to the strike of the main slope at Handcar Peak, is likely to be stable. Field observations support this, because mass wasting from the scarp appears to be limited mainly to rockfall.

Although this kinematic analysis is useful for explaining small surficial instabilities at Handcar Peak, it may have limited application to the deep-seated deformation of the rock mass. At the scale of the entire deforming rock mass, the slope angle is not steep enough to allow significant toppling. Large-scale sliding is also unlikely as a primary mechanism of deformation – discontinuities daylight in 10-50-m-high outcrops, but sliding on these surfaces only provides local, surficial kinematic release. Figure 5 shows that the base of the overall deforming mass must have a shallower orientation. Perhaps the base of the deformation is a series of dispersed shear zones that grade downward into more competent rock (Stewart 1997). Movement may also occur along the joints by means of a more complex step-path mechanism, dying out at the depth where the confinement mobilizes sufficient frictional strength to prevent slip.

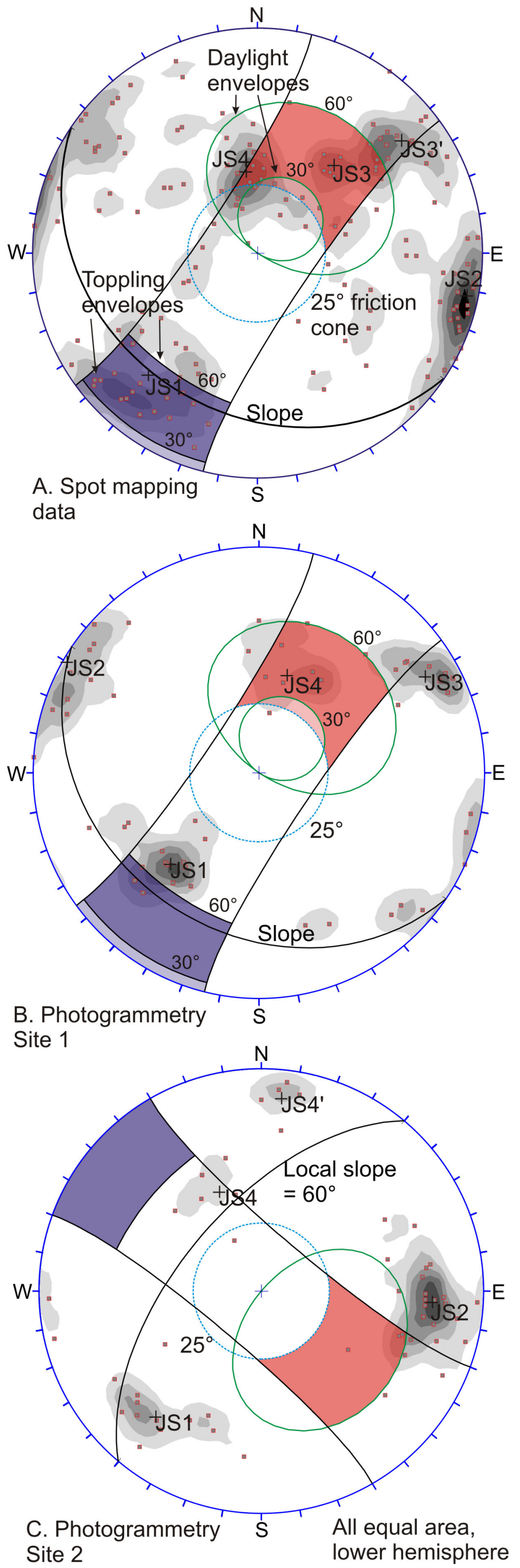

Figure 8. Discontinuity data and kinematic analysis for (A) and (B) the main slope of the Handcar Peak DsGSD and locally steep outcrops, and (C) the Buck Creek scarp. A 25 degree friction angle was used.

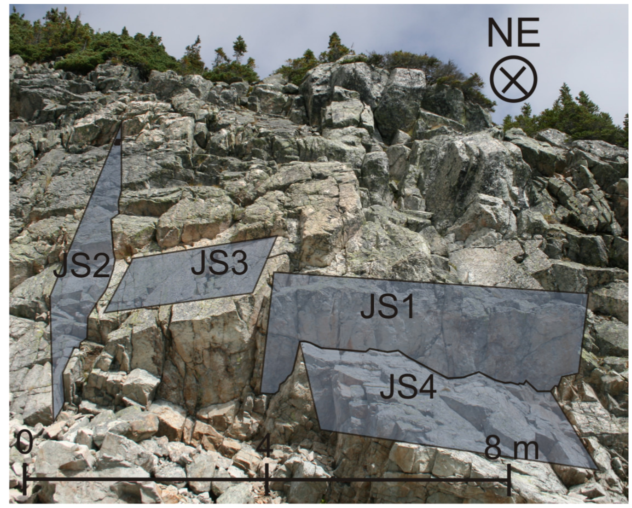

Figure 9. Prominent joint sets at photogrammetry site 1. GSI here is 50-60 (block size 4000-48000 cm3)

5.5 Numerical modeling

The distinct element code UDEC (Itasca Consulting Group, 2008) was selected to model the deforming rock mass at Handcar Peak. UDEC's explicit time-marching solution scheme can model slow, progressive movement that accumulates displacements over time but may never progress to catastrophic failure. In addition, the high intact rock strength and organized discontinuity structure dictate the use of a discontinuum approach.

A preliminary model geometry was created from the profile shown in Figure 5, extending from the top of Caboose Mountain to the floor of the Lillooet Valley. To avoid boundary effects, the model was extended to the sides and below the profile. A zero velocity condition in the x direction was imposed on the lateral boundaries, and the lower boundary was fixed in the y direction. In-situ horizontal stresses were initialized as 0.5 times the magnitude of vertical stresses (K=0.5).

An elastoplastic Mohr-Coulomb constitutive model was assigned to the rock mass. Debuttressing of the slope during deglaciation was simulated by assigning properties of glacier ice to the material above the slope profile and removing it from the 2000-m-deep valley in five stages. Discontinuity shear strength was then lowered to explore model response to conditions of high pore water pressures at the time of deglaciation and seasonally during snowmelt. Model properties are shown in Table 1. Rock mass properties were derived using the program RocLab (RocScience 2007) with data from point load index tests and a GSI of 60. Joint strength properties are based on published values for strong intrusive rocks and clay-filled faults. Figure 10 illustrates the displacement patterns produced with two different joint configurations after 50,000 model cycles.

Table 1. Joint and rock mass properties used in UDEC models.

Joint Properties	Rock Joints	Relict Faults
Normal Stiffness (MPa/m)	1000	500
Shear Stiffness (MPa/m)	100	50
φ°	25	16
Cohesion (kPa)	500	100
Tensile Strength (kPa)	0	0
Rock Mass Properties[1]	GSI = 60	
ρ (g/cm^3)	2.8	
Bulk Modulus (Gpa)	38.1	
Shear Modulus (Gpa)	22.9	
Poisson's Ratio	0.3	
Tensile Strength (MPa)	1.5	
φ °	46	
Cohesion (MPa)	14.5	
Dilation angle °	5	

[1]From RocLab

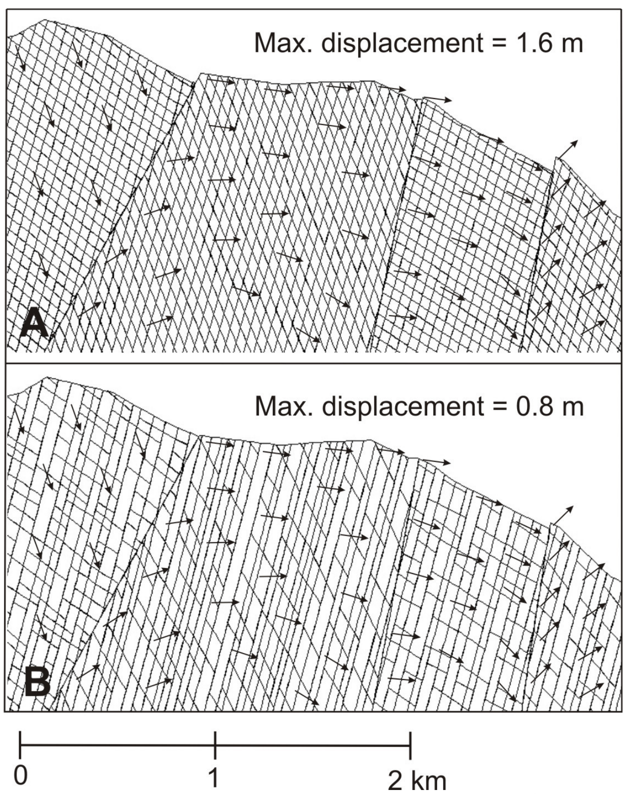

Figure 10. Displacements in preliminary UDEC model with: (A) JS3 discontinuities fully persistent, (B) JS3 discontinuities not fully persistent. Block deformation exaggerated 50x.

Although the pattern of displacement vectors is similar for the two models, the magnitude of displacement is greater where the discontinuities in set JS3 are assumed to be fully persistent. This configuration in UDEC is less realistic geometrically, but may more accurately portray the ability for movement to take place by step-path linking of small-scale fractures. The joint configuration in Figure 9B is somewhat more realistic, but results in a rock mass that is kinematically constrained from experiencing slip on discontinuity surfaces. Further modeling will explore additional joint networks and constitutive behavior.

Because this study is extremely data-limited, these preliminary UDEC models serve primarily as a conceptual experiment to aid in understanding potential DSGSD failure mechanisms at Handcar Peak. The results show good agreement with the concept that deformation of the rock mass will be preferentially accommodated along the weak fault planes that are expressed at the surface as antislope scarps and trenches. Formation of antislope scarps is reproduced in the two UDEC models as the slope deforms downwards. Below the lowermost antislope scarp, the rock mass moves upward and outward, reproducing the bulging toe of the DSGSD.

6 CONCLUSIONS

The extensive network of linear surface features at Handcar Peak is characteristic of a large deforming rock mass. Movement probably began with the retreat of valley glaciers during deglaciation when the oversteepened valley sides were debuttressed. Geomorphic evidence indicates that the failure has been retrogressive; the tall lower antislope scarps are now stable, whereas activity continues near the upper end of the deforming rock mass. Movement in the upper portion of the DSGSD has been slow and relatively steady throughout the Holocene, with 0.5 m of movement occurring on one linear in the past 2400 years. The existing joint structure appears to be unfavorable for kinematic failure involving simple sliding or toppling. Instead, a more complex mechanism is indicated, one involving elastoplastic deformation of the rock mass with displacements preferentially accommodated along relict tectonic faults.

ACKNOWLEDGEMENTS

This work was supported by NSERC Discovery Grants to Clague and Stead. We thank Marco Giardino and David Van Zeyl for their help and guidance in the initial stages of the project.

REFERENCES

ADAM Technology. 2007. 3DM analyst 2.1, 3DM CalibCam 2.1. http://www.adamtech.com.au.

Ambrosi, C. and Crosta, G. B. 2006. Large sackung along major tectonic features in the central italian alps; large landslides; dating, triggering, modelling, and hazard assessment. *Engineering Geology, 83*(1-3): 183-200.

Ballantyne, C. K. 2002. Paraglacial geomorphology. *Quaternary Science Reviews, 21*(18-19): 1935-2017.

Bovis, M. J. and Evans, S. G. 1996. Extensive deformations of rock slopes in southern Coast Mountains, southwest British Columbia, Canada. *Engineering Geology, 44*(1-4): 163-182.

Clague, J. J., Evans, S. G., Rampton, V. N., and Woodsworth, G. J. 1995. Improved age estimates for the White River and Bridge River tephras, western Canada. *Canadian Journal of Earth Sciences, 32*(8): 1172-1179.

Hoek E, Carranza-Torres CT, Corkum B. 2002. The Hoek-Brown failure criterion-2002 edition. In: *Proceedings of the 5th North American Rock Mechanics Symposium*, Toronto, Canada. Vol. 1:267-273.

International Society of Rock Mechanics. 1978. Suggested methods for the quantitative description of discontinuities in rock masses. *International Journal of Rock Mechanics and Mining Sciences & Geomechanics Abstracts*, *15*(6): 319-368.

Itasca Consulting Group. 2009. UDEC modelling code version 4.01. http://www.itascacg.com/udec/index.php.

Lund, M. 2002. Anti-slope scarp investigation at Handcar Peak, British Columbia, Canada. Undergraduate thesis, Lund University, Lund, Sweden, 28 pp.

McCalpin, J. P. 1999. Criteria for determining the seismic significance of sackungen and other scarplike landforms in mountainous regions. *Ridge-top spreading in California: California Geological Survey Open File Report*.

Monger, J. W. H. and Journeay, J. M. 1994. Geology of the southern coast and intermontane belt. *Geological Survey of Canada Open File Report 2490*, scale 1:500,000.

Rocscience Inc. 2007. RocLab version 1.031. http://www.rocscience.com.

Savage, W. Z. and Varnes, D. J. 1987. Mechanics of gravitational spreading of steep-sided ridges. *Bulletin of the International Association of Engineering Geology, 35*(1): 31-36.

Soldati, M. 2004. Deep-seated gravitational slope deformation. In A. S. Goudie (Ed.), *Encyclopedia of geomorphology,* pp. 226-228

Stewart, T. W. G. 1997. Investigation of rock-slope deformation at the Wahleach hydroelectric project using the FLAC computer code. M.Sc. thesis, University of British Columbia, Vancouver, BC, 320 pp.

Sturzenegger, M. and Stead, D. 2009. Close-range terrestrial digital photogrammetry and terrestrial laser scanning for discontinuity characterization on rock cuts. *Engineering Geology, 106*(3-4): 163-182.